Combining Ultra-High Drug-Loaded Micelles and Injectable Hydrogel Drug Depots for Prolonged Drug Release

Michael M. Lübtow, Thomas Lorson, Tamara Finger, Florian-Kai Gröber-Becker, and Robert Luxenhofer*

Hydrogel-based drug depot formulations are of great interest for therapeutic applications. While the biological activity of such drug depots is often characterized well, the influence of incorporated drug or drug-loaded micelles on the gelation properties of the hydrogel matrix is less investigated. However, the latter is of great importance from fundamental and application points of view as it informs on the physicochemical interactions of drugs and water-swollen polymer networks and it determines injectability, depot stability, as well as drug-release kinetics. Here, the impact of incorporated drug, neat polymer micelles, and drug-loaded micelles on the viscoelastic properties of a cytocompatible hydrogel is investigated systematically. To challenge the hydrogel with regard to the desired application as injectable drug depot, curcumin (CUR) is chosen as a model compound due to its very low-water solubility and limited stability. CUR is either directly solubilized by the hydrogel or pre-incorporated into polymer micelles. Interference of CUR with the temperature-induced gelation process can be suppressed by pre-incorporation into polymer micelles forming a binary drug delivery system. Drug release from a collagen matrix is studied in a trans-well setup. Compared to direct injection of drug formulations, the hydrogel-based systems show improved and extended drug release over 10 weeks.

M. M. Lübtow, Dr. T. Lorson,[+] Prof. R. Luxenhofer
Functional Polymer Materials
Chair for Advanced Materials Synthesis
Department of Chemistry and Pharmacy and Bavarian Polymer Institute
University of Würzburg
Röntgenring 11, 97070 Würzburg, Germany
E-mail: robert.luxenhofer@uni-wuerzburg.de

T. Finger, Dr. F.-K. Gröber-Becker
Translational Center 'Regenerative Therapies' (TLC-RT) Fraunhofer
Institute for Silicate Research (ISC)
Neunerplatz 2, 97082 Würzburg, Germany

Dr. F.-K. Gröber-Becker
Chair of Tissue Engineering and Regenerative Medicine
University Hospital Würzburg
Röntgenring 11, 97070 Würzburg, Germany

The ORCID identification number(s) for the author(s) of this article can be found under https://doi.org/10.1002/macp.201900341.

[+]Present address: Institute of Pharmacy and Food Chemistry, Julius-Maximilians-University Würzburg, Am Hubland, 97074 Würzburg, Germany

1. Introduction

Once administered into the human body, a drug faces various challenges before reaching its target location. Drug delivery systems such as liposomes or polymer nanoparticles/micelles are utilized to protect the drug but any circulating system is also challenged to a certain degree by excretion and/or biotransformation in the human body.[1] Control of pharmacokinetics and pharmacodynamics is particularly important and challenging when administering readily metabolized compounds. Another important aspect for drug delivery systems is the drug release kinetics. As intrinsically dynamic systems, drug-loaded polymer micelles often face the challenge of rapid drug release, which then associates with proteins present in the blood stream[2,3]; is excreted, or taken up in tissue other than desired one, which may be detrimental for the therapeutic efficacy.[4] To enable a more sustained release, active pharmaceutical ingredients (API) can be embedded in drug depots from which the drug is released continuously, maintaining a high local drug concentration in the surrounding tissue over an extended period of time.[5–7] Ideally, the depot formulation not only prolongs drug release, but also protects the incorporated compound from premature degradation. Besides microfabricated devices,[8] metallic implants,[9] organogels[10] or electrospun fibers,[11] hydrogels[12] are considered promising drug depot matrices. Hydrogels are three-dimensionally cross-linked networks of water-soluble polymers.[13,14] Due to their high water content, hydrogels are generally regarded as highly biocompatible.[15,16] Drug-loaded hydrogels as depot formulations showed great therapeutic potential in various scenarios in vitro[17–21] as well as in vivo.[22–29] *In situ* forming or injectable hydrogels are of particular interest due to their ease of application without surgical needs.[30–33] In this context, physically crosslinked thermogelling hydrogels based on hydrophobic interactions are advantageous, as they can be injected in the cold, liquid state to solidify at body temperature without the addition of crosslinkers or any other external trigger.[34,35] Various compounds including PTX,[36] interleukin-2,[37] topotecan,[38] doxorubicin,[25] or fluorouracil[39] have been incorporated into thermogelling hydrogels to prolong drug release as well as enhance retention at tumor site.

A compound which is particularly challenging to formulate—in form of hydrogels or otherwise—is curcumin (CUR). A plethora of preclinical studies pointed out the antioxidative,[40] cardioprotective,[41] or antitumor[42] activities of the "generally recognized as safe" (GRAS; evaluated by United States Food and Drug Administration (FDA))[43] compound. Despite a large number of clinical trials, it has not been approved as drug for human use. Besides potentially troublesome evaluation of preclinical data,[44–47] this is most likely associated with the extremely low water solubility of 0.6 mg L^{-1} (1.6 µM)[48] of CUR as well as the molecules' high susceptibility to degradation, not only in water,[49,50] but also to biomedical transformations such as carbon chain cleavage, reduction, conjugation with glucuronic acid or sulfate in biological media in vitro[51] and in vivo.[52] These issues make CUR an interesting model compound to challenge hydrogels with respect to their desired application as injectable drug depot. Previously, poly(2-oxazoline) (POx) and poly(2-oxazine) (POzi)-based drug-delivery vehicles with interesting structure–property relationships with respect to drug loading and potential for parenteral administration of CUR were reported.[53–58] The loading capacities (LCs) for CUR in ABA triblock-copolymers comprising the same hydrophilic poly(2-methyl-2-oxazoline) (PMeOx) corona (= A) and either poly(2-n-butyl-2-oxazoline) (PBuOx) (= A-BuOx-A) or (poly(2-n-propyl-2-oxazine) (PPrOzi) (= A-PrOzi-A) as hydrophobic blocks ranged from 21.6 wt% to 54.5 wt%.[53] Although benefits with respect to therapeutic efficacy of intravenously administered, ultra-high loaded A-BuOx-A/ paclitaxel formulations (LC = 45 wt%) and combination formulations of hydrophobic cis-platin prodrug and etoposide or PTX have been observed in vivo,[59–63] this might not be true for CUR due to its susceptibility to degradation or toxicity at high concentrations (not achievable orally). Inspired by CUR-loaded hydrogels for cutaneous wound repair[28] or intranasal drug delivery to the brain,[64] we wondered, if we could incorporate CUR in a recently reported, cytocompatible PMeOx-b-PPrOzi copolymer-based hydrogel,[65] for subcutaneous or intratumoral injection in order to avoid systemic circulation and/or allow prolonged release. From a more fundamental and practical point of view, it was also interesting to investigate the influence of hydrophobic CUR on the viscoelastic properties of a hydrogel that is formed based on dynamic hydrophobic interactions. Furthermore, the effect of nanoformulated CUR incorporated into the hydrogel matrix is of interest. Although drug-loaded polymer micelles incorporated into hydrogel matrices are readily found in the literature,[17,28,29,66] such systematic investigations of the viscoelastic properties of hydrogels containing nanoformulated hydrophobic drugs are rare. In addition, to assess the potential as an injectable thermogelling drug depot, the CUR-loaded hydrogels were injected into a collagen matrix and CUR release quantified.

2. Experimental Section

2.1. Reagents and Solvents

All substances used for the preparation of polymers were purchased from Sigma-Aldrich (Steinheim, Germany) or Acros (Geel, Belgium) and were used as received unless otherwise stated. Curcumin powder from Curcuma longa (turmeric)

was purchased from Sigma-Aldrich and analyzed in-house (curcumin = 79%; demethoxycurcumin = 17%, bisdemethoxycurcumin = 4%; determined by HPLC analysis; Figure S18, Supporting Information). Deuterated chloroform (CDCl$_3$) or methanol (MeOD) for NMR analysis was obtained from Deutero GmbH (Kastellaun, Germany).

The monomers 2-n-propyl-2-oxazine (nPrOzi), 2-n-butyl-2-oxazoline (nBuOx) and 2-n-butyl-2-oxazine (nBuOzi) were synthesized according to Seeliger et al.[67] (Figures S1–S4, Supporting Information). All substances used for polymerization, namely methyl trifluoromethylsulfonate (MeOTf), propargyl p-toluenesulfonate, benzonitrile (PhCN), sulfolane and all monomers were refluxed over CaH$_2$ (PhCN was refluxed over P$_2$O$_5$) and distilled under argon.

2.2. Polymer Synthesis

The polymerizations and work-up procedures of the ABA triblock-copolymers[54] as well as the AB diblock-copolymers[65] were described recently and can be found in Figures S5–S16, Supporting Information. Briefly, the preparation of block-copolymers was performed as follows: initiator was added to a dried and nitrogen flushed flask and dissolved in the respective amount of solvent. The monomer for the first block was added and the reaction mixture was heated to 100 °C (2-R-2-oxazoline) or 120 °C (2-R-2-oxazine). Reaction progress was controlled by FTIR- and ^{1}H-NMR-spectroscopy. After complete monomer consumption, the mixture was cooled to RT and the monomer for the second block was added. After complete monomer consumption, the procedure was repeated for the third block in the case of ABA triblock-copolymers. After monomer consumption was confirmed for the last block, termination was carried out by addition of a secondary amine at 50 °C for 4 h. Subsequently, K$_2$CO$_3$ was added and the mixture was stirred at 50 °C for 4 h. Precipitates were removed by centrifugation and the solvent was removed under reduced pressure. The supernatant was transferred into a dialysis bag and dialyzed against Millipore water overnight. The solution was recovered from the bag and lyophilized.

2.3. Nuclear Magnetic Resonance Spectroscopy

^{1}H-NMR spectra were recorded on a Fourier 300 (300 MHz), Bruker Biospin (Rheinstetten, Germany) at 298 K. The spectra were calibrated to the signal of residual protonated solvent signal (CDCl$_3$: 7.26 ppm). Multiplicities of signals are depicted as follows: s, singlet; d, doublet; t, triplet; q, quartet; quin, quintet; dt; doublet of triplets; m, multiplet; b, broad.

2.4. Dialysis

Dialysis was performed using Spectra/Por membranes with a molecular weight cutoff of 1 kDa (ABA-triblock copolymers) or 8 kD (AB-diblock copolymers) (material: cellulose acetate) obtained from neoLab (Heidelberg, Germany). Water (Millipore) was renewed after 1 and 4 h, and every 12 h subsequently, until end of dialysis.

**ADVANCED
SCIENCE NEWS**

www.advancedsciencenews.com

**Macromolecular
Chemistry and Physics**

www.mcp-journal.de

2.5. Gel Permeation Chromatography

Gel permeation chromatography (GPC) was performed on an Agilent 1260 Infinity System, Polymer Standard Service (Mainz, Germany) with either HFIP containing 3 g L^{-1} potassium trifluoroacetate; precolumn: 50 × 8 mm PSS PFG linear M; 2 columns: 300 × 8 mm PSS PFG linear M (particle size 7 µm) or DMF containing 1 g L^{-1} LiBr; precolumn: 50 × 8 mm PSS GRAM; columns: 30 and 1000 Å 300 × 8 mm PSS GRAM (particle size 10 µm) as eluent. The columns were kept at 40 °C and flow rates were 1.0 mL min^{-1} (DMF) or 0.7 mL min^{-1} (HFIP). Prior to each measurement, samples were filtered through 0.2 µm PTFE filters, Roth (Karlsruhe, Germany). Conventional calibration was performed with PEG standards (0.1–1000 kg mol^{-1}) and data were processed with WinGPC software.

2.6. CUR-Loaded Polymer Micelles

CUR-loaded polymer micelles were prepared by thin film method.[59] Ethanolic polymer (20 g L^{-1}) and CUR (5.0 g L^{-1}) stock solutions were mixed in desired ratio. After complete removal of the solvent at 50 °C under a mild stream of argon, the films were dried in vacuo (≤ 0.2 mbar) for 20 min. Subsequently, preheated (37 °C) H$_2$O was added. Complete solubilization was facilitated by shaking the solutions at 1250 rpm at 55 °C for 12 min with a Thermomixer comfort, Eppendorf AG (Hamburg, Germany). Non-solubilized drug (if any) was removed by centrifugation for 5 min at 9.000 rpm with a MIKRO 185 (Hettich, Tuttlingen, Germany). Solubilization experiments were performed with three individually prepared samples and results are presented as mean ± standard deviation (SD).

CUR quantification was performed by UV–vis absorption on a BioTek Eon Microplate Spectrophotometer, Thermo Fisher Scientific (MA, USA) using a calibration curve obtained with known amounts of CUR (Figure S19, Supporting Information). Samples were prepared in Rotilabo F-Type 96 well plates, Carl Roth GmbH & Co. KG (Karlsruhe, Germany) at a constant volume of 100 µL. Spectra were recorded from 300–600 nm at 25 °C and CUR was quantified at 428 nm. Prior to UV–vis absorption measurements, the aqueous formulations were appropriately diluted with ethanol. The following equations were used to calculate LC and loading efficiency (LE):

$$LE = \frac{m_{drug}}{m_{drug, added}} \qquad (1)$$

$$LC = \frac{m_{drug}}{m_{drug} + m_{polymer}} \qquad (2)$$

where m_{drug} and $m_{polymer}$ are the weight amounts of solubilized drug and polymer excipient in solution and $m_{drug,added}$ is the weight amount of drug initially added to the dispersion. No loss of polymer during micelles preparation was assumed.

2.7. CUR-Loaded Hydrogels

CUR-loaded hydrogels were prepared using a modified thin film method. Dried CUR/polymer films were dissolved in precooled (5 °C) H$_2$O (Millipore) and shaken at 1200 rpm at 8 °C with a Thermomixer comfort, Eppendorf AG (Hamburg, Germany) until no solids were detectable anymore by visual inspection (≈6 h). The clear, viscous solutions were used without further purification. For CUR quantification, small amounts of CUR-loaded hydrogels were sampled and dissolved in ethanol. Drug content was determined by UV–vis absorption according to Equation (3):

$$CUR(mg/g) = \frac{m_{drug}}{m_{hydrogel,wet}} \qquad (3)$$

where m_{drug} is the weight amount of solubilized drug and $m_{hydrogel,wet}$ is the weight of CUR-loaded hydrogel in the wet state. Loading capacity LC was determined according to Equation (2). For the determination, three samples were taken from the respective hydrogel and measured individually. However, each hydrogel was prepared once.

2.8. Incorporation of CUR-Loaded Polymer Micelles into Hydrogel

Respective amounts of freeze-dried, CUR-loaded polymeric micelles were added to a precooled (≈8 °C) aqueous solution of the respective hydrogel (20 wt%). The dispersion was gently shaken at ≈8 °C until the freeze-dried micelles were completely dissolved in the hydrogel solution (≈2 days). The drug contents of the clear, highly viscous solutions were determined according to Equation (8) and LC was determined according to Equation (2).

2.9. Rheology

Rheological analysis was performed on a Physica MCR 301, Anton Paar (Ostfildern, Germany) utilizing a plate–plate geometry (diameter 25 mm). The rheometer was equipped with a Peltier element. Prior to temperature-sweep measurements, the samples were allowed to equilibrate on the rheometer at 5 °C for 3 min. Following this, the temperature was raised linearly from 5 to 60 °C at 5 °C min^{-1}. Frequency was 1 Hz and the amplitude was 0.5% at 0.5 mm plate–plate distance. Within these conditions, the hydrogels (20 wt% in deionized H$_2$O) were within their linear viscoelastic region[65] and CUR-loaded hydrogels were assumed to be as well.

2.10. HPLC Measurements

CUR-loaded hydrogels were analyzed on a LC-20A Prominence HPLC, Shimadzu (Duisburg, Germany) equipped with a system controller CBM-20A, a solvent delivery unit LC-20 AT (double plunger), an online degassing unit DGU-20A, an autosampler SIL-20AC, and a SPD-20A UV–vis detector. As stationary phase, a ZORBAX Eclipse Plus, Agilent (Santa Clara,

1900341 (3 of 13)

CA, USA) C18 column (4.6 × 100 mm; 3.5 µm) was used. The mobile phase was a gradient of H_2O/ACN (Figure S18a, Supporting Information) at 40 °C and a flow rate of 1 mL min^{-1}. CUR was quantified at 427 nm. Possible degradation products were investigated at 220 nm.

2.11. Long-Term Stability Studies

For long-term stability studies, CUR-loaded hydrogels were stored in the freezer (≈8 °C). For CUR quantification, small amounts of CUR-loaded hydrogels were sampled and dissolved in ethanol. Drug content was determined by UV–vis absorption at 428 nm. To confirm CUR integrity, small amounts of CUR-loaded hydrogels were sampled and diluted with ACN/H_2O = 60/40 (v/v) and characterized by HPLC analysis at 220 and 427 nm.

2.12. CUR-Release Studies

For CUR-release studies, CUR-loaded hydrogels were injected into trans-well inserts (24-well plate, BRANDplates insert system, BRAND GmbH & Co. KG, Wertheim, Germany) filled with collagen hydrogels at a final concentration of 6 g L^{-1} as reported previously[68] with a Hamilton syringe (injection volume: 10 µL). For every sample, three injection of the same batch of formulation were placed in individual wells. To ensure constant injection depth and position, a 3D-printed scaffold was utilized as guidance for the syringe. Prior to injection, the CUR-loaded hydrogel filled Hamilton syringe was cooled in the freezer (≈8 °C) to ensure liquidity of respective hydrogels. Basolateral chamber was filled with 1500 µL PBS and collagen matrix in the apical side was covered with 100 µL PBS. At specific time-points mentioned in main text, the solution of the basolateral side was removed, freeze-dried and dissolved in ethanol. Ethanolic solutions were centrifuged for 10 min at 9000 rpm in order to avoid scattering from undissolved salts from PBS. CUR content of the supernatant was quantified by UV–vis absorption at 428 nm and CUR integrity confirmed by HPLC analysis at 220 and 427 nm.

3. Results and Discussion

3.1. CUR Solubilization

Whereas A-BuOx-A nanoformulations exhibit CUR LCs comparable to those found in the literature for other polymer amphiphiles (LC ≈20 wt%[69]), its structural isomer A-PrOzi-A enables very high CUR-loadings >50 wt%.[54] The drug formulations with these ABA-triblock copolymers are designed for intravenous (IV) administration; however, rapid clearance of APIs in highly dynamic polymer micelles has been observed.[60] In contrast, steady serum concentrations, which can be crucial in many applications, could be achieved through the use of subcutaneous depots.[70] In 2017, Lorson et al. reported a POx/POzi-based reversibly thermogelling hydrogel as cytocompatible bioink.[65] As this polymer comprises the same building

Table 1. Analytical data of investigated block copolymers including the yield, molar mass M_n and dispersity $Đ$.

Composition[a]	Polymer ID	Yield [%]	M_n[a]	M_n[b]	M_n[c]	$Đ$[c]
				[kg mol^{-1}]		
PMeOx$_{35}$-b-PPrOzi$_{20}$-b-PMeOx$_{35}$	A-PrOzi-A	67	8.7	9.8*	6.1	1.16
PMeOx$_{35}$-b-PBuOx$_{20}$-b-PMeOx$_{35}$	A-BuOx-A	82	8.6	7.0*	7.2	1.18
PMeOx$_{35}$-b-PBuOzi$_{20}$-b-PMeOx$_{35}$	A-BuOzi-A	67	9.0	9.4*	5.6	1.20
PPrOzi$_{50}$-b-PMeOx$_{50}$	H50	75	10.8	10.4**	7.3	1.17
PPrOzi$_{100}$-b-PMeOx$_{99}$	H100	89	21.3	20.2**	10.4	1.38

[a]According to [M]$_0$/[I]$_0$; [b]Obtained by ^{1}H-NMR (*CDCl$_3$; **MeOD); evaluated as mean of all relevant signals; [c]Obtained by GPC (eluent: DMF, calibrated with PEG standards); deviations in molar mass determination between NMR end-group analysis and GPC standard calibration can be attributed to the use of PEG-standards for calibration.[55] Synthesis and characterization of the triblock-[54] as well as diblock-copolymers[65] was previously reported.

blocks as A-PrOzi-A but has a different architecture (AB diblock vs ABA triblock) and monomer ratio, the effects of solubilized CUR on the hydrogel properties (gel temperature, storage/loss modulus) are of interest. Hence, CUR was incorporated into aqueous solutions of PPrOzi$_{50}$-b-PMeOx$_{50}$ (H50) and PPrOzi$_{100}$-b-PMeOx$_{99}$ (H100) (**Table 1**; for polymer synthesis and characterization, the reader is referred to Figures S12–S16, Supporting Information). Such, the influence of the degree of polymerization (DP) of both blocks on the solubilization capacity for CUR can be assessed.

Although exhibiting the same building blocks as A-PrOzi-A, both diblocks exhibited much lower LCs for CUR than the former as well as compared to A-BuOzi-A and A-BuOx-A. At 10 g L^{-1} polymer, only 0.87 g L^{-1} (LC = 8 wt%) or 0.91 g L^{-1} (8.4 wt%) CUR could be solubilized using H50 or H100, respectively (**Figure 1**a). Increasing the polymer concentration to 50 g L^{-1} somehow increased CUR loadings up to 15 wt% (CUR = 8.8 g L^{-1}) in the case of H50. Similar shortcoming of AB diblock-copolymers compared to the corresponding ABA triblock-copolymers with respect to their solubilization capacity has been observed before. Whereas A-BuOx-A exhibits LCs up to 49 wt% for the water-insoluble drug paclitaxel (PTX), the corresponding diblock only enabled PTX-loadings of 17 wt%.[71] However, in this case, the DP of the respective blocks were similar while in the present case the thermoresponsive block has a much higher DP in the diblocks compared to the triblock. At ≤50 g L^{-1}, neither H50 nor H100 forms a gel, but apparently, the self-assemblies formed -presumably polymersomes-[72] are not well suited for CUR solubilization.[65]

The polymer concentrations of 10 and 50 g L^{-1} were chosen to compare the solubilization behavior of H50 or H100 with those of the previously reported A-BuOx-A, A-PrOzi-A, and A-BuOzi-A. The latter were designed as drug vehicles for intravenous administration, for which those moderate polymer concentrations are most suitable. In contrast, drug-loaded hydrogels find applications often at much higher polymer concentrations. Therefore, LC of H100 was also investigated at polymer concentrations of 20 wt% at which gelation occurs. As H100 already forms a gel <20 °C at this concentration the dried drug/polymer films were re-dispersed with water at 5 °C until no solid particles were detectable anymore by visual
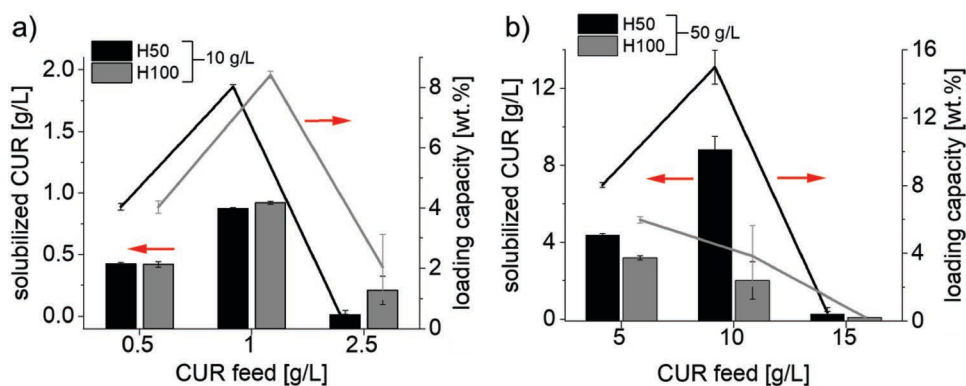
Figure 1. Solubilized aqueous CUR concentrations (bars, left axis) and corresponding loading capacities (lines, right axis) in dependence of the CUR feed by H50 (black) or H100 (gray) at polymer concentrations of a) 10 or b) 50 g L^{-1}. Data are given as means ± SD ($n = 3$).

inspection (≈6 h). The obtained clear solutions were moderately viscous at $T \leq 5$ °C and showed an increasing viscosity with increasing CUR loading, as per visual inspection. As defined volumes could not be easily sampled from the viscous solutions even at $T \leq 5$ °C, small amounts of the CUR-loaded hydrogels were weighed, and the CUR loading will be defined as the ratio of solubilized CUR (mg) with respect to the total weight of the hydrogel in the hydrated state (g) (Equation (3)). Loading

efficiencies (LE) between 75% and 83% and rather high aqueous CUR concentrations of up to 23.6 ± 0.5 mg/g (LC = 10.6 wt%) at mass concentration of $\rho(\text{H100}) = 20$ wt% (**Figure 2**a) could be obtained. The fact that those high CUR concentrations were feasible using H100 and because H50 only gelled at elevated temperature with ($T_{\text{gel}} > 57$ °C) or without ($T_{\text{gel}} = 40$ °C) the addition of triblock copolymers (Figure S20, Supporting Information), H50 was not investigated further in the present work. It should
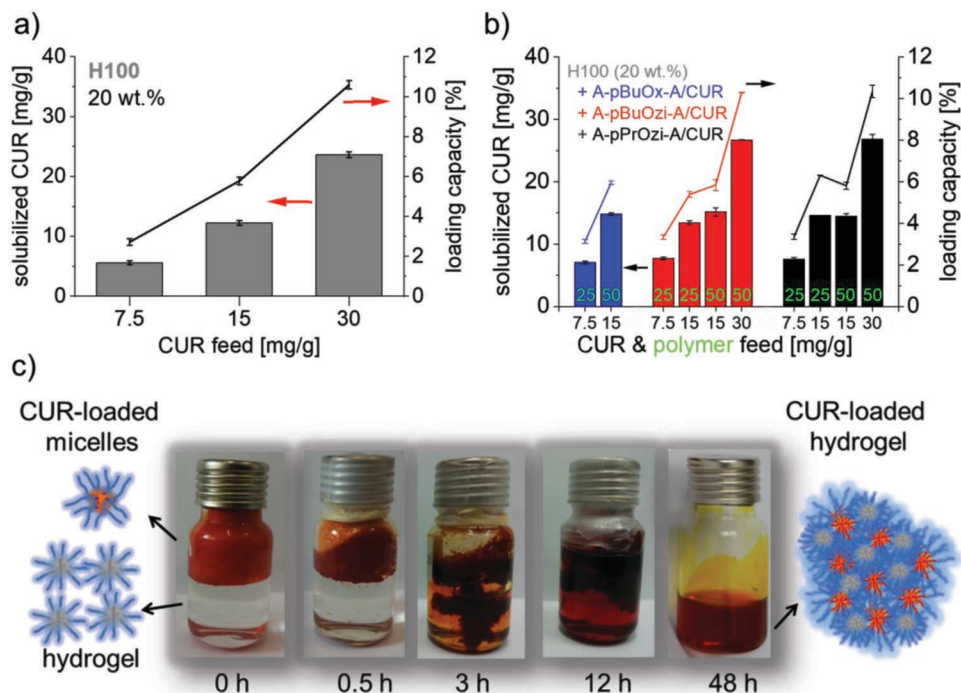

Figure 2. a) Solubilized aqueous CUR concentrations (bars, left axis) and corresponding loading capacities (line, right axis) in dependence of the CUR feed by H100 at 20 wt% in H$_2$O. Data are given as means ± SD ($n = 3$); b) solubilized aqueous CUR concentrations (bars, left axis) and corresponding loading capacities (lines, right axis) in dependence of the CUR feed by H100 (20 wt% in H$_2$O) after incorporation of freeze-dried, CUR-loaded micelles of either A-BuOx-A (blue), A-BuOzi-A (red), or A-PrOzi-A (black). Amount of polymer within the CUR-loaded micelles was either 25 mg/g$_{\text{hydrogel,wet}}$ or 50 mg/g$_{\text{hydrogel,wet}}$ (green). Each hydrogel was prepared once; however, CUR concentration was quantified with three withdrawn samples each to confirm homogeneous CUR distribution and absence of precipitation; c) images of the incorporation of freeze-dried, CUR-loaded micelles (A-PrOzi-A/CUR = 50/30 g/g) into H100 (20 wt% in H$_2$O). The amounts of A-PrOzi-A and CUR were 50 and 15 mg/g, respectively. Samples were gently shaken at 5 °C for 2 days. Illustration of CUR-loaded micelles and (CUR-loaded) gels, are given as a very rough visualization and should not be confused with the actual structure of the respective solutions.
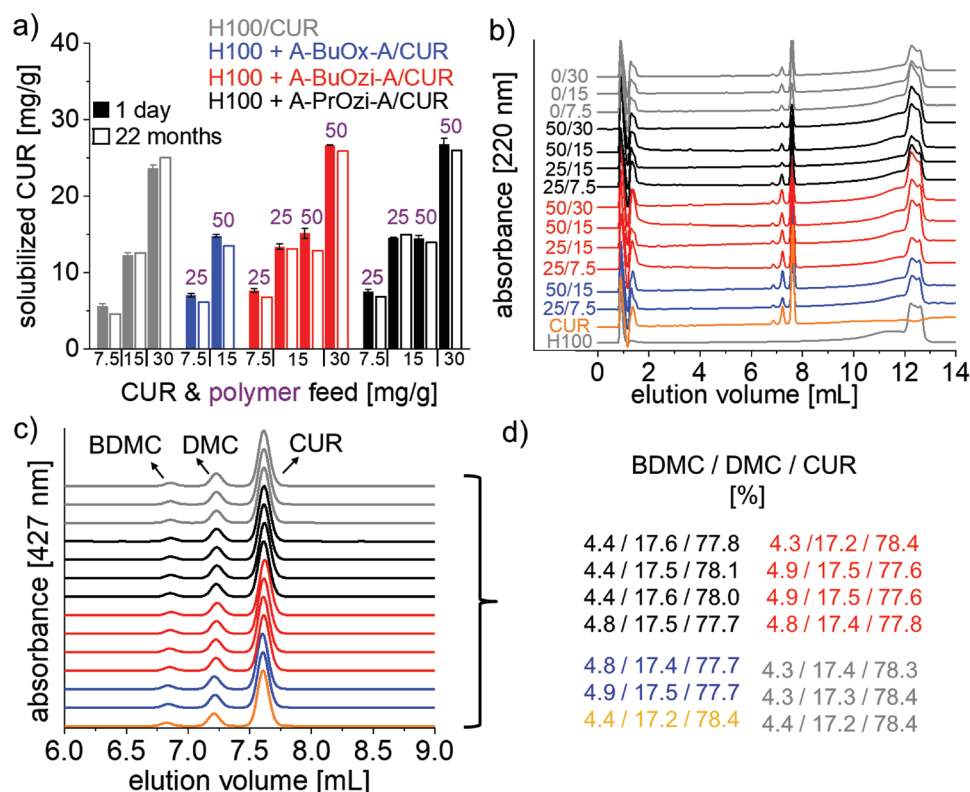
Figure 3. a) Solubilized aqueous CUR concentrations in dependence of the CUR feed (*x*-axis) by H100 (20 wt% in H$_2$O) after preparation (full bars) or 22 months storage at 8 °C under the exclusion of light (hollow bars). CUR was either directly solubilized by H100 (gray) or pre-incorporated into polymer micelles of A-BuOx-A (blue), A-BuOzi-A (red), or A-PrOzi-A (black). Concentration of the ABA triblock-copolymers is given by purple numbers (mg/g$_{hydrogel,wet}$); b) corresponding HPLC elugrams after 22 months storage at λ_{abs} = 220 nm to exclude CUR degradation. Elugrams of neat H100 (bottom, gray) and CUR (2nd bottom, orange) are given for comparison. Numbers left of the elugrams correspond to amount of ABA triblock-copolymer/CUR (mg/g$_{hydrogel,wet}$); c) detailed view of the HPLC elugrams at λ_{abs} = 427 nm as well as d) corresponding ratio of BDMC, DMC, and CUR.

be noted that reproducibility of T_{gel} of H50 is generally more susceptible to batch-to-batch variations compared to H100.[65]

In addition to direct solubilization of CUR with H100, freeze-dried CUR nanoformulation of either A-BuOx-A (Figure 2b, blue), A-BuOzi-A (red) or A-PrOzi-A (black) were incorporated at same CUR feed concentrations of 7.5, 15, and 30 mg/g. To obtain more detailed insights into the influence of the ABA-triblock copolymers, two different triblock concentrations (25 and 50 mg/g) were investigated. Due to the limited LC of A-BuOx-A for CUR, highly loaded micelles were only feasible using A-BuOzi-A or A-PrOzi-A. The aqueous solutions of H100 (20 wt% in H$_2$O) were precooled to 5 °C and the respective amount of lyophilized, CUR nanoformulation was added. The mixture was shaken at 5 °C for 2–4 days (depending on the used polymer and CUR concentration) until a completely clear and viscous solution was formed (Figure 2c). Similar to the solubilization of neat CUR (Figure 2a), the hydrogels incorporating CUR-loaded micelles exhibited excellent LEs >95% (Figure 2b) with no visible sign of precipitation.

The CUR-loaded hydrogels showed even higher stability than the CUR nanoformulations of, for example, A-PrOzi-A[54] and drastically prolonged shelf-life with no apparent loss of CUR-content even after 22 months of storage in the sol-state at 8 °C under the exclusion of light (**Figure 3**a).

This is remarkable, as 90% of CUR was reported elsewhere to be degraded in water (pH = 7.2; 37 °C) after 30 min.[49,50] Although exhibiting high polymer concentrations up to 25 wt% (H100 = 20 wt% + ABA triblock copolymer = 5 wt%), the major component of the CUR-loaded hydrogels remains water. Important to note, the prolongation of the aqueous CUR solubility was observed irrespective whether CUR was directly solubilized by H100 (Figure 3a, gray bars) or incorporated as nanoformulation (blue, red, black bars). Furthermore, this remarkable long-term stability was found irrespective of the chemical structure of the triblock copolymers. Similarly, an extraordinary suppression of crystallization was previously observed in nanoformulations of paclitaxel using A-BuOx-A.[71] HPLC analysis suggests that no CUR degradation occurred as the ratio between the curcuminoids bisdemethoxycurcumin (BDMC), demethoxycurcumin (DMC) and CUR remained constant during 22 months storage (Figure 3b,c) which reportedly shifts during degradation processes.[73] Hennink and co-workers previously reported that polymer micelles can stabilize CUR in water by several orders of magnitude, but they still clearly observed degradation within a few days.[69] As all samples showed comparable loading and long-term stabilities, the rheological properties of all CUR loaded hydrogels were determined as described in the following.
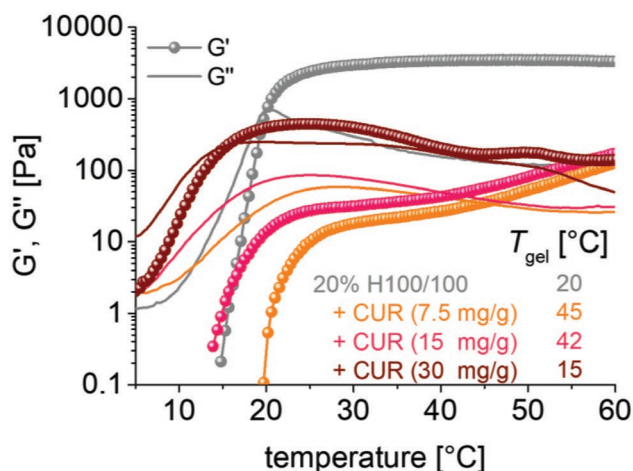
ADVANCED
SCIENCE NEWS
www.advancedsciencenews.com

Macromolecular
Chemistry and Physics
www.mcp-journal.de

Figure 4. Temperature dependent rheological analysis of H100 (20 wt%) before (gray) and after solubilization of 7.5 (orange), 15 (pink) or 30 (brown) mg/g CUR. Samples were heated from 5 to 60 °C at 5 °C min⁻¹. Frequency was 1 Hz at 0.5% amplitude. T_{gel} is defined as the crossover of storage G' (lines with symbols) and loss modulus G'' (lines without symbols).

3.2. Rheological Properties

3.2.1. CUR-Loaded Hydrogels

Addition of hydrophobic CUR strongly affected the thermoresponsive and viscoelastic properties of H100-based hydrogels (**Figure 4**). Especially at low CUR feed concentrations of 7.5 or 15 mg/g, T_{gel} significantly increased from 20 °C (neat H100; 20 wt%) to 45 and 42 °C, respectively. Accordingly, the storage modulus (G') at 37 °C strongly decreased several magnitudes from 3.4 kPa (0 mg/g CUR) to 24 Pa (7.5 mg/g) and 39 Pa (15 mg/g). Clearly, incorporation of CUR significantly weakened the gel structure at same strain. Arguably, both trends are disadvantageous for the intended use as injectable drug depot, as T_{gel} should be below body temperature forming a gel with sufficient strength to prevent rapid dissolution/dispersion of the depot. A decrease in G' to 253 Pa (37 °C) was also observed at 30 mg/g CUR feed, whereas T_{gel} decreased to 16 °C. However, this gel remained rather weak with pronounced viscous character as the loss factor (tan $\delta = G''/G'$) remained close to unity. In any case, CUR clearly interferes significantly with the formation of a physically crosslinked polymer network necessary for gelation.

Similar trends of decreasing gel stiffness with increasing drug-content were also observed for other hydrogels such as poly-(D,L-lactic acid-co-glycolic acid) (PLGA)-polyethylene glycol (PEG)-PLGA.[27] In this report, G'_{max} ($T \approx 35$ °C) decreased from 520 to 280 and 250 Pa by incorporation of 0, 4, and 8 g L⁻¹ docetaxel (DTX), respectively. It should be mentioned that a dramatic decrease of G' to essentially 0 Pa at $T > 37$ °C occurred for both, the neat as well as the DTX-loaded hydrogel. Nevertheless, a single intratumoral injection of DTX-containing hydrogel was as efficient as three IV injections of DTX. In a different report, a decrease in maximum viscosity (η_{max}, 37 °C) with increasing drug content for

doxorubicin (0.6 g L⁻¹ DOX)[25] as well as PTX (2 g L⁻¹ PTX)[26] loaded PEG-b-polycaprolactone (PEG-PCL)-based hydrogels was observed. In another report, the gelation of PLGA-PEG-PLGA was completely prevented by the incorporation of 1.6 g L⁻¹ rapamycin. Interestingly, this strong interference could be suppressed by co-solubilization of two other hydrophobic drugs, paclitaxel and tanespimycin (17-AAG).[22] While the incorporation of hydrophobic drugs in various hydrogels consistently decreased gel stiffness, the influence on T_{gel} appeared to be rather small without a trend, as T_{gel} sometimes slightly increased,[19,25,26] and sometimes slightly decreased.[27]

However, we wondered if CUR addition in form of CUR nanoformulations[54] could prevent the detrimental interference with the gel, retaining the initial viscoelastic properties of H100.

3.2.2. Incorporation of ABA Triblock Copolymers into Hydrogel Matrix

Prior to the incorporation of CUR nanoformulations, the influence of the ABA triblock copolymers alone on the gelation properties of H100 is of interest. At low polymer concentrations of 25 mg/g hydrogel, only minor changes of the thermogelling properties of H100 occurred (**Figure 5**a). In the case of A-BuOzi-A and A-PrOzi-A, T_{gel} slightly increased to 23 and 25 °C respectively, whereas it remained constant in the case of A-BuOx-A. In case of A-PrOzi-A, the storage modulus (G') was reduced somewhat throughout the investigated temperature range ($G' = 2.2$ kPa (37 °C)), whereas it increased slightly through the incorporation of polymers bearing butyl side chains. The increase was most pronounced for A-BuOx-A with $G' = 4.7$ kPa (37 °C). The trend of decreasing T_{gel} and increasing gel stiffness became more prominent with increasing A-BuOx-A concentration. At A-BuOx-A = 50 mg/g, G' increased by a factor of two to 6.8 kPa (37 °C) (Figure 5b). T_{gel} decreased further to 17 °C, whereas G' kept increasing to 7.8 kPa (37 °C) when 100 mg/g A-BuOx-A were added (Figure 5c). At this point, the total polymer concentration was 27 wt%. However, the decrease in T_{gel} and increase of G' was not simply due to an increase in solids content, as shown in the case of A-BuOzi-A and A-PrOzi-A. At both, 50 and 100 mg/g triblock copolymer concentration, A-BuOzi-A as well as A-PrOzi-A increased T_{gel} and decreased gel stiffness (Figure 5b,c). This was most pronounced for A-PrOzi-A. As the latter comprises the same building blocks as H100, it seems reasonable that A-PrOzi-A interfered most with the gelation of H100. As both, hydrophilic and hydrophobic block are identical and the degree of polymerization does not differ very much, these two polymers should be expected to mix freely. Since the self-assembly of block copolymers does strongly depend on the block volume ratio, this must be expected to affect the self-assembly and thus, thermogelation of H100. A-BuOzi-A, sharing the same backbone but bearing a more hydrophobic central B block still interferes significantly, albeit somewhat less with the gelation of H100. Even though being intermediate with respect to hydrophobicity, A-BuOx-A exhibits an entirely different influence on the thermogelation of H100. At this point, we can only assume that the different backbone (POx vs POzi) of the hydrophobic block reduces mixing,
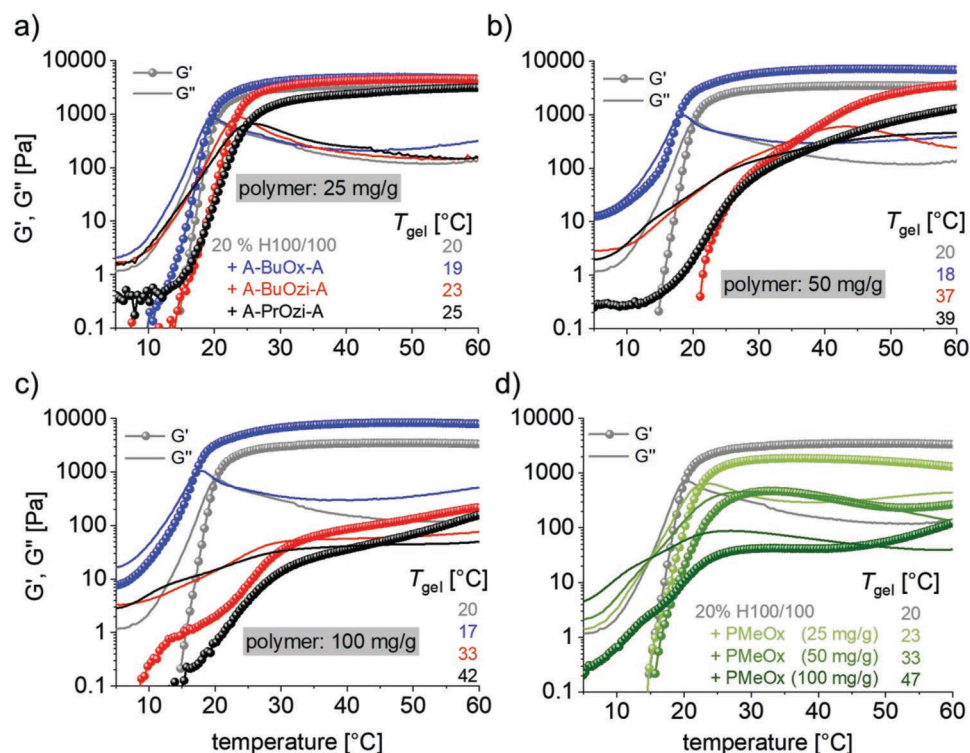
ADVANCED
SCIENCE NEWS

www.advancedsciencenews.com

Macromolecular
Chemistry and Physics

www.mcp-journal.de

Figure 5. Temperature dependent rheological analysis of H100 (20 wt%) before (gray) and after addition of a) 25; b) 50; or c) 100 mg/g of A-BuOx-A (blue), A-BuOzi-A (red), or A-PrOzi-A (black); d) incorporation of PMeOx homopolymer (DP = 30) at the same polymer concentration as it would be present by the incorporation of ABA triblock-copolymers at 25, 50, and 100 mg/g. Samples were heated from 5 to 60 °C at 5 °C min^{-1}. Frequency was 1 Hz at 0.5% amplitude. T_{gel} is defined as the intersection of storage G' (lines with symbols) and loss modulus G'' (lines without symbols).

and therefore, does not influence network formation of H100 as much. The lower T_{gel} and higher G' may be explained by macromolecular crowding and competition for water molecules for hydration. Similarly, T_{gel} of thermoresponsive Pluronic F127 gel (18 wt%) also decreased from 27.4 to 25.8 and 23.1 °C when incorporating 0.21%, 0.42%, and 1.24% w/v phospholipid-based liposomes, respectively.[17] This was attributed to dehydration of F127 micellar cores due to entrapment of water in the inner hydrophilic core of the liposomes leading to a greater extend of dehydration and lower T_{gel}.

Important to note, A-BuOx-A, being the only polymer to decrease T_{gel} and increase G', was also the only ABA triblock copolymer exhibiting a thermogelling behavior on its own, albeit only at 20 wt%, and rather high temperatures T_{gel} = 41 °C. Also, the resulting gel was very weak with a low G' ($G'_{50\,°C}$ = 180 Pa) (Figure S21, Supporting Information). As a control to test the macromolecular crowding hypothesis, we also investigated the influence of PMeOx homopolymer with a DP of 100, approximately corresponding to the overall length of the ABA block copolymers. PMeOx was incorporated into H100 at the same concentrations as it is present incorporating the respective triblock copolymers at 25, 50, and 100 mg/g (Figure 5d). Interestingly, the PMeOx exhibited a weakening effect very similar to the one of A-PrOzi-A, yielding comparable temperature-dependent rheological profiles, sol–gel transition temperatures as well as gel stiffnesses. This, in combination with the difference between PMeOx and, for example, A-BuOx-A once more highlights the influence of the hydrophobic block

of the respective triblock copolymers. Next, it was interesting to investigate how the incorporation of CUR nanoformulations of the different triblock copolymers affect the thermoresponsive behavior of H100.

3.2.3. Incorporation of CUR Nanoformulations of ABA Triblock Copolymers into Hydrogel Matrix

In contrast to neat CUR or neat polymers, the incorporation of CUR and polymer in form of nanoformulations of A-BuOx-A, A-BuOzi-A, or A-PrOzi-A affected the viscoelastic properties to a lesser extent (**Figure 6**). Overall, T_{gel} was either comparable or lower than that of neat H100 (20 wt%). This suggests that the CUR nanoformulations remain largely intact during their dissolution in H100. Having a distinct core–shell structure in mind, all CUR loaded micelles present the same hydrophilic PMeOx corona, somehow masking the influence of the different hydrophobic cores (Figure 5a–c).

That such core–shell structure is probably not a fully accurate representation of the actual micellar morphology becomes evident when considering the remaining small differences between the hydrogels incorporating different CUR nanoformulations suggesting a small but noticeable effect of the hydrophobic block on the hydrogel properties. We recently reported that in fact the hydrophilic corona is involved in the binding of CUR in this system.[74] Similar to the incorporation of the neat triblock copolymers, A-BuOx-A/CUR exhibited the highest gel
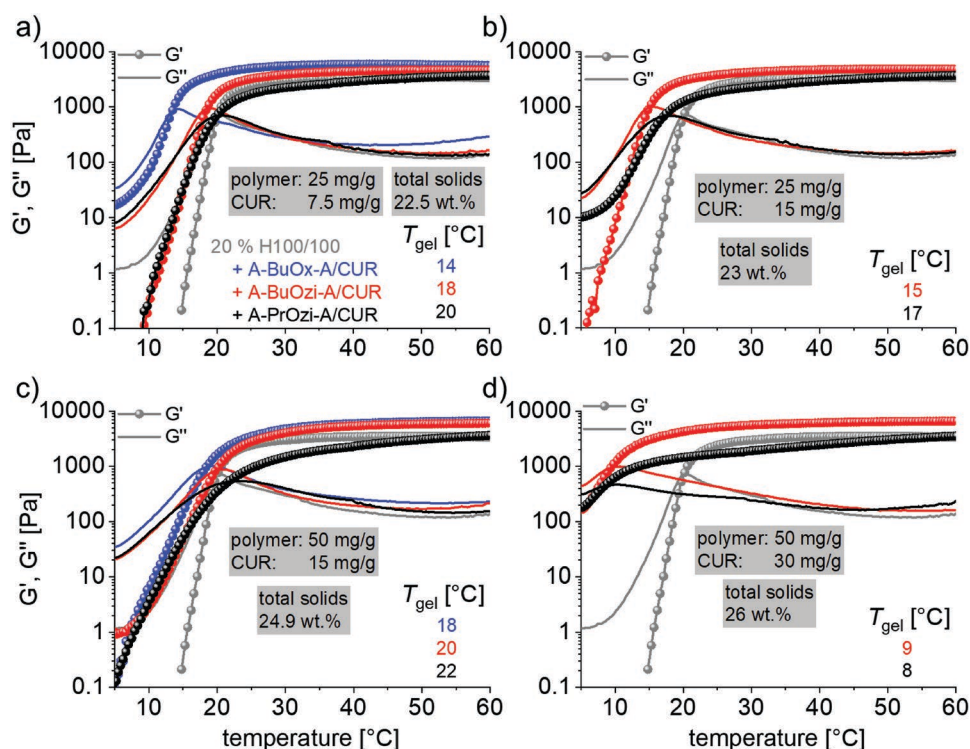
**ADVANCED
SCIENCE NEWS**
www.advancedsciencenews.com

**Macromolecular
Chemistry and Physics**
www.mcp-journal.de

Figure 6. Temperature dependent rheological analysis of H100 (20 wt%) before (gray) and after incorporation of CUR-loaded polymer micelles of A-BuOx-A (blue), A-BuOzi-A (red), or A-PrOzi-A (black). Concentration of polymer/CUR added was either a) 25/7.5; b) 25/15; c) 50/15; or d) 50/30 mg/$g_{H100,wet}$. Samples were heated from 5 to 60 °C at 5 °C min^{-1}. Frequency was 1 Hz at 0.5% amplitude. T_{gel} is defined as the intersection of storage G' (lines with symbols) and loss modulus G'' (lines without symbols).

stiffness at a given temperature, whereas G' of A-PrOzi-A/CUR was still below that of neat H100.

To verify the reproducibility of our observations, we synthesized a second batch of H100 and investigated its rheological properties (Figure S22a, Supporting Information). More importantly, also the influence of A-PrOzi-A/CUR at both, the lowest (25/7.5 mg/$g_{H100,wet}$; Figure S22b, Supporting Information) and highest solids content (50/30 mg/$g_{H100,wet}$, Figure S22c, Supporting Information), was highly reproducible using the different batch of H100. A-PrOzi-A/CUR was either added as dry powder to 20 wt% H100 (as employed above) or added as highly concentrated aqueous solution (A-PrOzi-A/CUR = 150/90 or 75/22.5 g/L) to 30 wt% H100 to yield the same final polymer, CUR and hydrogel concentrations. Although the latter preparation method is faster, aqueous polymer/drug concentrations of 150/90 g/L may not be generally feasible with most systems.

The differences between the various nanoformulations were also apparent by the flow properties of the respective hydrogels, as H100 + A-BuOx-A/CUR exhibited shape integrity already at 15 °C, whereas A-BuOzi-A/CUR or A-PrOzi-A/CUR were free-flowing sols under the same conditions (**Figure 7**a), despite rheological analysis might suggest otherwise ($G' < G''$ for all samples at 15 °C, Figure 7b). Nevertheless, all hydrogels incorporating CUR nanoformulations exhibited sol–gel transitions well below body temperature as well as sufficient stability at 37 °C, making them promising candidates as injectable drug depots. Therefore, the CUR release of selected hydrogels was investigated in the next step.

3.2.4. CUR Release from Hydrogels Embedded in Collagen

To investigate the CUR release under conditions related to the desired application as injectable, subcutaneous drug depot, the CUR-loaded hydrogels were injected into a collagen matrix embedded on the apical side of trans-well inserts and subsequently the CUR release determined on the basolateral side. Collagen was chosen since it reflects the composition and structure of human connective tissue to which drug-loaded hydrogels might be applied in a future clinical setting. In preliminary experiments, we noticed major variabilities in the drug release profile, which we attributed to variation of the positioning of the hydrogel depot within the collagen matrix. To reduce such variations, the syringes containing the CUR-loaded hydrogels were guided using a 3D-printed scaffold to ensure reproducible injection depth (0.25 cm at 0.5 cm height of collagen) as well as injection position (**Figure 8**a). Before injection, the syringes loaded with the respective hydrogels were cooled for 20 min at 8 °C to ensure liquidity of the respective sols. CUR was either neatly incorporated into the hydrogel (20 wt% H100 + 15 mg/g CUR) or in the form of A-PrOzi-A (polymer/CUR = 50/30 mg/g) or A-BuOx-A (polymer/CUR = 50/15 mg/g) nanoformulations, both at maximum CUR-loadings. These hydrogels were selected due to their different gel properties. Whereas H100 directly incorporating CUR exhibited a sol–gel transition above body-temperature (T_{gel} = 42 °C; $G'_{37°C}$ = 37 Pa; Figure 4), both hydrogels incorporating triblock-copolymers are solid gels at the investigated 37 °C (Figure 6c,d). Interestingly,
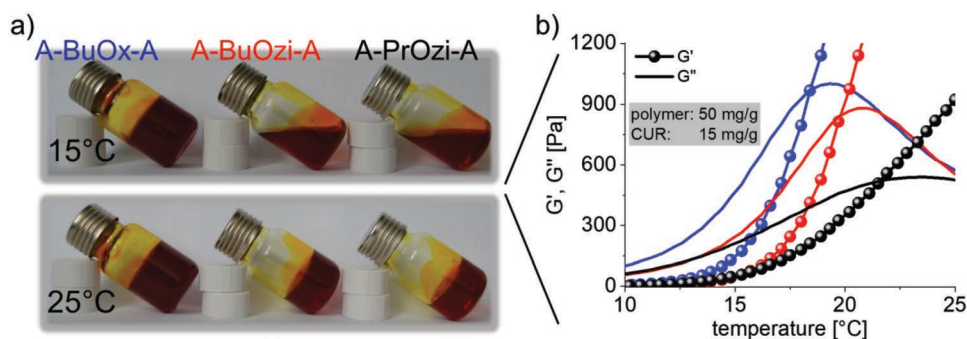
ADVANCED
SCIENCE NEWS
www.advancedsciencenews.com

Macromolecular
Chemistry and Physics
www.mcp-journal.de

Figure 7. a) Flow properties of H100 (20 wt% in H₂O) incorporating CUR-loaded polymeric micelles (polymer/CUR = 50/15 mg/g) at either 15 (top) or 25 °C (bottom); b) corresponding rheological properties of respective hydrogels.
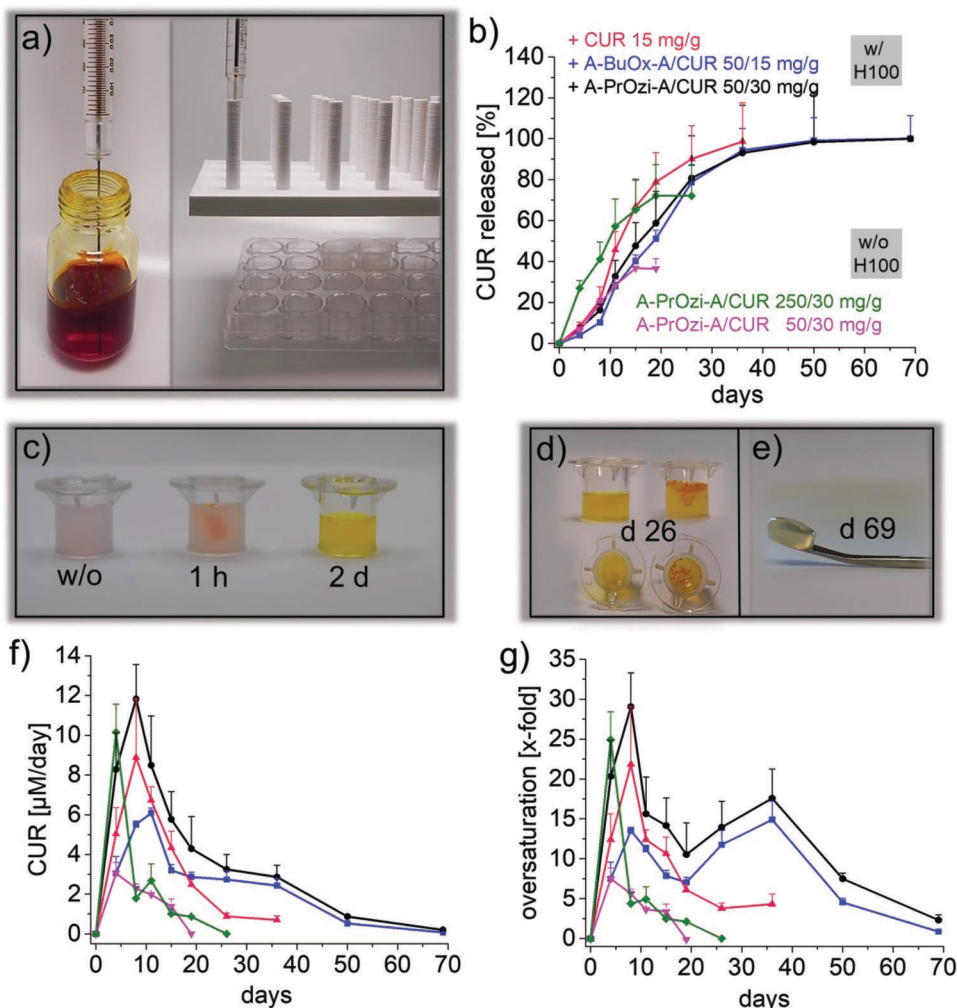

Figure 8. a) Setup for CUR release studies from CUR-loaded hydrogels or CUR-loaded polymer micelles injected into a collagen matrix. Hydrogel was added in a Hamilton syringe, cooled to 8 °C and subsequently injected (10 µL) into a transwell containing collagen. To ensure same injection depths and positions within the collagen matrix, the syringe was guided with a 3D printed scaffold (right picture); b) long-term CUR release of CUR directly incorporated into H100 (20 wt%; red curve) or pre-incorporated into either A-BuOx-A (polymer/CUR = 50/15 mg/g; blue curve) or A-PrOzi-A (polymer/ CUR = 50/30 mg/g, black curve). A-PrOzi-A/CUR at either polymer/CUR = 250/30 mg/g (green) or 50/30 mg/g (pink) without H100 for comparison; c) appearance of collagen matrix before (left) and 2 h (middle) or 2 days (right) after injection of H100/A-PrOzi-A/CUR (representative for all hydrogel containing samples); d) appearance of collagen containing H100/A-PrOzi-A/CUR (left) or A-PrOzi-A/CUR = 250/30 mg/g (right) after 26 days incubation in PBS; e) collagen matrix initially containing H100/A-PrOzi-A/CUR after release experiment (d 69); f) aqueous CUR concentration in basolatoral chamber released per day; g) concentration of released CUR with respect to CUR aqueous solubility (= oversaturation) at day of quantification. All CUR-loaded samples were prepared once and injected in three individual trans-wells containing collagen. Results are presented as mean ± SD (n = 3).

H100/CUR exhibited the fastest CUR-release of all samples (Figure 8b, red curve). Nevertheless, a sustained release was obtained with 50% CUR release after approximately 15 days ($t_{50\%}$). H100 incorporating A-BuOx-A/CUR at the same CUR concentration of 15 mg/g (blue curve) exhibited a slower release profile, with $t_{50\%} = 19$ days. This may be attributed to the much stronger network, as evidenced by their rheological properties ($G'_{37°C}$(H100/CUR) = 37 Pa; $G'_{37°C}$(H100/A-BuOx-A/CUR) = 5.7 kPa). The slower release in the presence of A-BuOx-A could also be due to altered pore sizes of the respective hydrogel which might to some extent correlate with the gel stiffness. To investigate this hypothesis, more detailed investigations utilizing, for example, fluorescence recovery after photobleaching would be necessary, which are outside the scope of the current contribution.

A more sustained release of acetylsalicylic acid (AS) pre-incorporated into lipid nanoparticles compared to directly solubilized AS also occurred for κ-carrageenan-based hydrogels within the first 2 h after immersing the respective hydrogels in water.[66] However in contrast to the presently reported findings, the cumulative release within 40 h of directly solubilized AS was much lower than that of formulated one reaching a plateau already after 15 h (= incomplete overall drug release). Unfortunately, the influence of the nanoformulation on gelation properties was not further investigated in this report. Similarly, Nie et al.[17] observed a prolonged release of PTX pre-incorporated into liposomes compared to solubilization of neat PTX with Pluronic F127 at both, the dialysis method (20% vs 40% release after 8 h) as well as when immersing the gels in water (60% vs 90% release after 8 h).

H100 incorporating A-PrOzi-A/CUR (Figure 8b, black curve) exhibited the longest release profile with 50% release after approximately 23 days and 80% release after 36 days. As the differences between H100 incorporating either A-PrOzi-A/CUR or A-BuOx-A/CUR became evident only at later stage of 19 days and after, the longer release of the former is probably due to the higher CUR concentration in the case of A-PrOzi-A/CUR rather than the viscoelastic properties of the hydrogel ($G'_{37°C}$(H100/A-PrOzi-A/CUR) = 2.0 kPa). A similar faster cumulative release at lower drug-loading was also observed for PEG-PCL-PEG-based hydrogels when immersed at 37 °C in PBS.[75] At 1 g L^{-1} honokiol, 45% drug was released after 8 days, whereas only 35% were released at 2 g L^{-1} in the same time period. Cumulative release of honokiol reached a plateau already at day 8 with little less than 50% overall release after 14 days, hinting toward drug crystallization/precipitation preventing further release. However, the release studies in this report were only performed once and conclusions should be regarded with great care. In accordance with the previous observations, a slower drug release also occurred for PLGA-PEG-PLGA-based hydrogels incorporating increasing amounts of DTX.[27] Cumulative drug release after 3 weeks at 37 °C were 92% and 85% at 2 and 8 g L^{-1} DTX, respectively. Similarly, cumulative release from PEG-PCL hydrogel was slower at 2 g L^{-1} PTX (30% after 30 days) than at 1 g L^{-1} (40% after 30 days).[26]

Important to note, the CUR release from the drug-loaded hydrogels was essentially quantitative with overall CUR releases of ≥98%. In contrast, when injecting neat A-PrOzi-A/CUR nanoformulations into collagen without incorporation into H100 at either the same nanoformulation concentration as present in H100 hydrogel (50/30 mg/g; pink curve) or at the same total polymer concentration (hydrogel + nanoformulation, 250/30 mg/g; green curve), a strikingly different release profile occurred. At the latter, CUR release was fastest with half-life of 10 days. The slower CUR release at lower A-PrOzi-A concentration of 50 mg/g (pink curve) may be attributed to a non-homogenous distribution in the collagen matrix or a smaller excess of polymer carrier. Whereas A-PrOzi-A/CUR = 250/30 mg/g enabled a decent overall release of 72%, only 36% of total added CUR was released from A-PrOzi-A/CUR = 50/30 mg/g. Visual inspection of the respective collagen samples revealed the reason for this incomplete release in the absence of H100. Immediately after injection, a more or less spherical depot is discernable at the injection site (Figure 8c, 1 h). After day 1, the yellow color of CUR distributed homogenously throughout the whole collagen matrix (Figure 8c, 2 days). This homogeneity remained throughout the whole release experiment in all samples containing H100. In contrast, without H100, precipitation of CUR occurred at a later stage (Figure 8d, right sample) correlating with the incomplete CUR release (Figure 8b, green and pink curves). This is quite interesting, as the nanoformulation A-PrOzi-A/CUR itself exhibits excellent stability in aqueous media.[54] This suggests that the collagen matrix somehow destabilizes the nanoformulations while this was apparently not the case when using H100/CUR depots. This is of great importance regarding the desired application as injectable drug depot, as it enables sustained and complete release over long periods of time. Important to note, after the release experiments, as suggested by the quantitative analysis, all collagen matrices initially containing H100 were completely colorless showing no sign of retained CUR (Figure 8e).

Important to note, only the CUR release of A-pPrOzi-A/CUR directly incorporated into collagen without H100 showed a linear release profile at early timepoints (followed by plateau region) when plotted against square root of time (Figure S23b, Supporting Information). A linear trend is typical of the Fickian diffusion mechanism.[76] In contrast, when incorporated into H100, a sigmoidal CUR release was observed (Figure S23a, Supporting Information). The deviation from the often observed linear square root release kinetic of small compounds incorporated into hydrogel matrices might be due to the dual hydrogel system, that is, incorporation of drug-loaded hydrogel (H100) into another hydrogel (collagen). In case of the neat nanoformulations, the maximum CUR concentrations released per day were already reached at day 4 (Figure 8f). In contrast, employing H100 depots, released CUR concentration gradually increased up to day 8 (H100/CUR; H100/A-PrOzi-A/CUR) or day 11 (H100/A-BuOx-A/CUR), respectively, before they started to decrease. This can be attributed to the reduced diffusivity in H100, prolonging the homogenous distribution of the respective gels in the collagen matrix. CUR concentrations well above CUR aqueous solubility of 1.6 μM (0.6 mg L^{-1}[48]) were reached in all samples in the recipient chamber. Therefore, we must assume that CUR was not released as free drug, but in solubilized form, presumably in the form of drug-loaded polymer micelles. In the case of the hydrogel incorporating A-PrOzi-A/CUR, a pronounced oversaturation with respect to

CUR aqueous solubility was achieved at day 11 ([CUR] = 47 μM, 29-fold, Figure 8g, black curve) and the oversaturation extended for several weeks (e.g., 18-fold at day 36) suggesting the long-term integrity of CUR nanoformulations in the collagen matrix. Important to note, the increase in CUR oversaturation from day 19 to day 36 is due to longer time intervals between sampling of the basolateral solution (Figure 8g, black and blue curves). In terms of controlled release, the drug depot featuring the A-BuOx-A/CUR showed arguably the most promising performance. The early-time concentration spike was less pronounced and quite steady release was observed over the course of 30 days.

4. Conclusion

CUR was incorporated into a cytocompatible hydrogel either directly or in form of a nanoformulation for a prospective injectable drug depot. Solubilization of neat CUR strongly interfered with the gelation of the hydrogel while incorporation of neat polymer used in nanoformulations resulted in two opposing trends. The purely POx-based triblock copolymer increased gel stiffness as well as decreased T_{gel}, whereas polymers bearing POzi-based hydrophobic cores similar or same to the one present in the hydrogel impeded the gelation process. Interestingly the influence of both, CUR and the neat polymers, was strongly attenuated by incorporating both into the hydrogel matrix in form of CUR nanoformulations suggesting that the drug-loaded polymer micelles remain largely intact within the POx-based hydrogel. After injection into a collagen matrix used as a simple model for subcutaneous administration, all POx-based systems exhibited essentially quantitative CUR-release. Interestingly, CUR directly incorporated into the hydrogel showed the fastest cumulative release, whereas the CUR nanoformulations exhibit markedly prolonged drug release. This is in accordance with their viscoelastic properties. Even after 50 days, the concentration of released CUR was above the inherent CUR water solubility, illustrating the release of CUR in a solubilized form from this novel combined drug depot and delivery systems. Most interestingly, CUR-loaded polymer micelles injected without hydrogel showed CUR precipitation in the collagen matrix. In contrast, collagen containing CUR-loaded POx hydrogels showed no sign of CUR precipitation during 69 days of release experiment. These findings together with the extraordinary shelf life of the CUR-loaded hydrogels with no loss of CUR-content even after 22 months make them an interesting platform as a combined drug depot and delivery system for, for example, subcutaneous or intraocular injections. As the presently investigated hydrogel has been demonstrated to be suitable as a bioink for 3D cell printing, we envision the combination of 3D cell bioprinting with 3D printed drug depots with extended release as potential future development.

Supporting Information

Supporting Information is available from the Wiley Online Library or from the author.

Conflict of Interest

M.M.L., T.L., and R.L are listed as inventors on patent applications pertinent to materials discussed in this contribution.

[1] D. E. Owens, N. A. Peppas, *Int. J. Pharm.* **2006**, *307*, 93.
[2] T. Kar, P. Basak, S. Sen, R. K. Ghosh, M. Bhattacharyya, *Front. Biol.* **2017**, *12*, 199.
[3] X. Yang, Z. Ye, Y. Yuan, Z. Zheng, J. Shi, Y. Ying, P. Huang, *Luminescence* **2013**, *28*, 427.
[4] S. Behzadi, V. Serpooshan, R. Sakhtianchi, B. Müller, K. Landfester, D. Crespy, M. Mahmoudi, *Colloids Surf., B* **2014**, *123*, 143.
[5] J. Li, D. J. Mooney, *Nat. Rev. Mater.* **2016**, *1*, 16071.
[6] N. A. Peppas, *Curr. Opin. Colloid Interface Sci.* **1997**, *2*, 531.
[7] P. I. Lee, C.-J. Kim, *J. Control. Release* **1991**, *16*, 229.
[8] C. L. Stevenson, J. T. Santini, R. Langer, *Adv. Drug Delivery Rev.* **2012**, *64*, 1590.
[9] J. A. Lyndon, B. J. Boyd, N. Birbilis, *J. Control. Release* **2014**, *179*, 63.
[10] A. Vintiloiu, J.-C. Leroux, *J. Control. Release* **2008**, *125*, 179.
[11] M. Chen, Y.-F. Li, F. Besenbacher, *Adv. Healthcare Mater.* **2014**, *3*, 1721.
[12] G. W. Ashley, J. Henise, R. Reid, D. V. Santi, *Proc. Natl. Acad. Sci. USA* **2013**, *110*, 2318.
[13] E. M. Ahmed, *J. Adv. Res.* **2015**, *6*, 105.
[14] M. Caldorera-Moore, N. A. Peppas, *Adv. Drug Delivery Rev.* **2009**, *61*, 1391.
[15] A. S. Hoffman, *Adv. Drug Delivery Rev.* **2012**, *64*, 18.
[16] M. K. Nguyen, D. S. Lee, *Macromol. Biosci.* **2010**, *10*, 563.
[17] S. Nie, W. L. W. Hsiao, W. Pan, Z. Yang, *Int. J. Nanomed.* **2011**, *6*, 151.
[18] X. J. Loh, B. J. H. Yee, F. S. Chia, *J. Biomed. Mater. Res., Part A* **2012**, *100A*, 2686.
[19] G. D. Kang, S. H. Cheon, S.-C. Song, *Int. J. Pharm.* **2006**, *319*, 29.
[20] A. Altunbas, S. J. Lee, S. A. Rajasekaran, J. P. Schneider, D. J. Pochan, *Biomaterials* **2011**, *32*, 5906.
[21] A. Almomen, S. Cho, C.-H. Yang, Z. Li, E. A. Jarboe, C. M. Peterson, K. M. Huh, M. M. Janát-Amsbury, *Pharm. Res.* **2015**, *32*, 2266.
[22] H. Cho, G. S. Kwon, *J. Drug Targeting* **2014**, *22*, 669.
[23] J.-J. Xuan, Y.-D. Yan, D. H. Oh, Y. K. Choi, C. S. Yong, H.-G. Choi, *Drug Delivery.* **2011**, *18*, 305.
[24] J. Y. Lee, K. S. Kim, Y. M. Kang, E. S. Kim, S.-J. Hwang, H. B. Lee, B. H. Min, J. H. Kim, M. S. Kim, *Int. J. Pharm.* **2010**, *392*, 51.

[25] Y. M. Kang, G. H. Kim, J. I. Kim, D. Y. Kim, B. N. Lee, S. M. Yoon, J. H. Kim, M. S. Kim, *Biomaterials* **2011**, *32*, 4556.

[26] S. Xu, W. Wang, X. Li, J. Liu, A. Dong, L. Deng, *Eur. J. Pharm. Sci.* **2014**, *62*, 267.

[27] Y. Gao, F. Ren, B. Ding, N. Sun, X. Liu, X. Ding, S. Gao, *J. Drug Targeting* **2011**, *19*, 516.

[28] C. Gong, Q. Wu, Y. Wang, D. Zhang, F. Luo, X. Zhao, Y. Wei, Z. Qian, *Biomaterials* **2013**, *34*, 6377.

[29] C. Ju, J. Sun, P. Zi, X. Jin, C. Zhang, *J. Pharm. Sci.* **2013**, *102*, 2707.

[30] A. Hatefi, B. Amsden, *J. Control. Release* **2002**, *80*, 9.

[31] A. Fakhari, J. Anand Subramony, *J. Control. Release* **2015**, *220*, 465.

[32] X. J. Loh, J. Li, *Expert Opin. Ther. Pat.* **2007**, *17*, 965.

[33] S. Kempe, K. Mäder, *J. Control. Release* **2012**, *161*, 668.

[34] M. A. Ward, T. K. Georgiou, *Polymers* **2011**, *3*, 1215.

[35] C. Gong, T. Qi, X. Wei, Y. Qu, Q. Wu, F. Luo, Z. Qian, *Curr. Med. Chem.* **2013**, *20*, 79.

[36] C. Ju, J. Sun, P. Zi, X. Jin, C. Zhang, *J. Pharm. Sci.* **2013**, *102*, 2707.

[37] W. E. Samlowski, J. R. McGregor, M. Jurek, M. Baudys, G. M. Zentner, K. D. Fowers, *J. Immunother.* **2006**, *29*, 524.

[38] G. Chang, T. Ci, L. Yu, J. Ding, *J. Control. Release* **2011**, *156*, 21.

[39] C. Gong, C. Wang, Y. Wang, Q. Wu, D. Zhang, F. Luo, Z. Qian, *Nanoscale* **2012**, *4*, 3095.

[40] T. Ak, İ. Gülçin, *Chem.-Biol. Interact.* **2008**, *174*, 27.

[41] S. Miriyala, M. Panchatcharam, P. Rengarajulu, in *The Molecular Targets and Therapeutic Uses of Curcumin in Health and Disease*, Springer, Berlin **2007**, pp. 359–377.

[42] X. Yang, Z. Li, N. Wang, L. Li, L. Song, T. He, L. Sun, Z. Wang, Q. Wu, N. Luo, C. Yi, C. Gong, *Sci. Rep.* **2015**, *5*, 10322.

[43] S. C. Gupta, S. Patchva, B. B. Aggarwal, *AAPS J.* **2013**, *15*, 195.

[44] M. A. W. Jonathan Baell, *Nature* **2014**, *513*, 481.

[45] M. Heger, *Nature* **2017**, *543*, 40.

[46] E. Burgos-Morón, J. M. Calderón-Montaño, J. Salvador, A. Robles, M. López-Lázaro, *Int. J. Cancer* **2010**, *126*, 1771.

[47] B. T. Kurien, S. P. Dillon, Y. Dorri, A. D'Souza, R. H. Scofield, *Int. J. Cancer* **2011**, *128*, 242.

[48] B. T. Kurien, A. Singh, H. Matsumoto, R. H. Scofield, *Assay Drug Dev. Technol.* **2007**, *5*, 567.

[49] Y.-J. Wang, M.-H. Pan, A.-L. Cheng, L.-I. Lin, Y.-S. Ho, C.-Y. Hsieh, J.-K. Lin, *J. Pharm. Biomed. Anal.* **1997**, *15*, 1867.

[50] M. Kharat, Z. Du, G. Zhang, D. J. McClements, *J. Agric. Food Chem.* **2017**, *65*, 1525.

[51] C. Schneider, O. N. Gordon, R. L. Edwards, P. B. Luis, *J. Agric. Food Chem.* **2015**, *63*, 7606.

[52] G. M. Holder, J. L. Plummer, A. J. Ryan, *Xenobiotica* **1978**, *8*, 761.

[53] M. M. Lübtow, L. Hahn, M. S. Haider, R. Luxenhofer, *J. Am. Chem. Soc.* **2017**, *139*, 10980.

[54] M. M. Lübtow, L. C. Nelke, J. Seifert, J. Kühnemundt, G. Sahay, G. Dandekar, S. L. Nietzer, R. Luxenhofer, *J. Control. Release* **2019**, *303*, 162.

[55] M. M. Lübtow, L. Keßler, A. Appelt-Menzel, T. Lorson, N. Gangloff, M. Kirsch, S. Dahms, R. Luxenhofer, *Macromol. Biosci.* **2018**, *18*, 1800155.

[56] E. Vlassi, A. Papagiannopoulos, S. Pispas, *Eur. Polym. J.* **2017**, *88*, 516.

[57] T. Lorson, M. M. Lübtow, E. Wegener, M. S. Haider, S. Borova, D. Nahm, R. Jordan, M. Sokolski-Papkov, A. V. Kabanov, R. Luxenhofer, *Biomaterials* **2018**, *178*, 204.

[58] Y. Milonaki, E. Kaditi, S. Pispas, C. Demetzos, *J. Polym. Sci., Part A: Polym. Chem.* **2012**, *50*, 1226.

[59] R. Luxenhofer, A. Schulz, C. Roques, S. Li, T. K. Bronich, E. V. Batrakova, R. Jordan, A. V. Kabanov, *Biomaterials* **2010**, *31*, 4972.

[60] Z. He, X. Wan, A. Schulz, H. Bludau, M. A. Dobrovolskaia, S. T. Stern, S. A. Montgomery, H. Yuan, Z. Li, D. Alakhova, M. Sokolsky, D. B. Darr, C. M. Perou, R. Jordan, R. Luxenhofer, A. V. Kabanov, *Biomaterials* **2016**, *101*, 296.

[61] X. Wan, Y. Min, H. Bludau, A. Keith, S. S. Sheiko, R. Jordan, A. Z. Wang, M. Sokolsky-Papkov, A. V. Kabanov, *ACS Nano* **2018**, *12*, 2426.

[62] X. Wan, J. J. Beaudoin, N. Vinod, Y. Min, N. Makita, H. Bludau, R. Jordan, A. Wang, M. Sokolsky, A. V. Kabanov, *Biomaterials* **2019**, *192*, 1.

[63] A. Zinger, L. Koren, O. Adir, M. Poley, M. Alyan, Z. Yaari, N. Noor, N. Krinsky, A. Simon, H. Gibori, M. Krayem, Y. Mumblat, S. Kasten, S. Ofir, E. Fridman, N. Milman, M. M. Lübtow, L. Liba, J. Shklover, J. Shainsky-Roitman, Y. Binenbaum, D. Hershkovitz, Z. Gil, T. Dvir, R. Luxenhofer, R. Satchi-Fainaro, A. Schroeder, *ACS Nano* **2019**, *13*, 11008.

[64] X. Chen, F. Zhi, X. Jia, X. Zhang, R. Ambardekar, Z. Meng, A. R. Paradkar, Y. Hu, Y. Yang, *J. Pharm. Pharmacol.* **2013**, *65*, 807.

[65] T. Lorson, S. Jaksch, M. M. Lübtow, T. Jüngst, J. Groll, T. Lühmann, R. Luxenhofer, *Biomacromolecules* **2017**, *18*, 2161.

[66] C. V. Kulkarni, Z. Moinuddin, Y. Patil-Sen, R. Littlefield, M. Hood, *Int. J. Pharm.* **2015**, *479*, 416.

[67] H. Witte, W. Seeliger, *Justus Liebigs Ann. Chem.* **1974**, *1974*, 996.

[68] C. Reuter, H. Walles, F. Groeber, in *3D Cell Culture, Methods in Molecular Biology*, Vol. *1612* (Ed: Z. Koledova), Humana Press, New York **2017**, p. 191.

[69] O. Naksuriya, S. Okonogi, R. M. Schiffelers, W. E. Hennink, *Biomaterials* **2014**, *35*, 3365.

[70] R. W. Moreadith, T. X. Viegas, M. D. Bentley, J. M. Harris, Z. Fang, K. Yoon, B. Dizman, R. Weimer, B. P. Rae, X. Li, C. Rader, D. Standaert, W. Olanow, *Eur. Polym. J.* **2017**, *88*, 524.

[71] Y. Seo, A. Schulz, Y. Han, Z. He, H. Bludau, X. Wan, J. Tong, T. K. Bronich, M. Sokolsky, R. Luxenhofer, R. Jordan, A. V. Kabanov, *Polym. Adv. Technol.* **2015**, *26*, 837.

[72] T. Lorson, *Ph.D. Thesis*, University of Würzburg **2019**.

[73] O. Naksuriya, M. J. van Steenbergen, J. S. Torano, S. Okonogi, W. E. Hennink, *AAPS J.* **2016**, *18*, 777.

[74] A.-C. Pöppler, M. M. Lübtow, J. Schlauersbach, J. Wiest, L. Meinel, R. Luxenhofer, *Angew. Chem.* **2019**, https://doi.org/10.1002/ange.201908914.

[75] C. Gong, S. Shi, P. Dong, B. Kan, M. Gou, X. Wang, X. Li, F. Luo, X. Zhao, Y. Wei, Z. Qian, *Int. J. Pharm.* **2009**, *365*, 89.

[76] E. Mauri, A. Negri, E. Rebellato, M. Masi, G. Perale, F. Rossi, *Gels* **2018**, *4*, 74.